BIOCHEMISTRY
including biophysical chemistry & molecular biology
Article

Biochemistry **2010,** *49,* 7783–7789 7783
DOI: 10.1021/bi100337p

Selection for Nonamyloidogenic Mutants of Islet Amyloid Polypeptide (IAPP) Identifies an Extended Region for Amyloidogenicity†

Ayano Fox,‡,∥ Thibaut Snollaerts,‡,∥ Camille Errecart Casanova,‡ Anastasia Calciano,‡ Luiza A. Nogaj,§ and David A. Moffet*,‡

‡*Department of Chemistry and Biochemistry, Loyola Marymount University, 1 LMU Drive, Los Angeles, California 90045, and* §*Department of Biology, Mount Saint Mary's College, Los Angeles, California 90049.* ∥*These authors contributed equally to this work.*

Received March 5, 2010; Revised Manuscript Received August 7, 2010

ABSTRACT: The aggregation of the 37-residue protein, islet amyloid polypeptide (IAPP), as either insoluble amyloid or as small oligomers, appears to play a direct role in the death of pancreatic β-islet cells in type II diabetes. While IAPP has been known to be the primary component of type II diabetes amyloid, the molecular interactions responsible for this aggregation have not been identified. To identify the aggregation-prone region(s), we constructed a library of randomly generated point mutants of IAPP. This mutant IAPP library was expressed in *Escherichia coli* as genetic fusions to the reporter protein enhanced green fluorescent protein (EGFP). Because IAPP aggregates rapidly, both independently and when fused to EGFP, the fusion protein does not yield a functional, fluorescent EGFP. However, mutations of IAPP that result in nonamyloidogenic sequences remain soluble and allow EGFP to fold and fluoresce. Using this screen, we identified 22 single mutations, 4 double mutations, and 2 triple mutations of IAPP that appear to be less amyloidogenic than wild-type human IAPP. A comparison of these sequences suggests residues 13 and 15−17 comprise an additional aggregation-prone region outside of the main amyloidogenic region of IAPP.

The aggregation of misfolded proteins into toxic oligomers and fibers has been linked to a variety of diseases such as type II diabetes, Alzheimer's disease, and Parkinson's disease. In type II diabetes the amyloid-forming peptide is islet amyloid polypeptide (IAPP,[1] amylin). This 37 amino acid polypeptide misfolds and forms aggregates within the pancreas. This misfolding into toxic aggregates, such as small soluble oligomers or large fibers, is believed to contribute to the loss of pancreatic β-cells. While the exact role of IAPP in type II diabetes is unclear, it is known that IAPP is found as extracellular deposits of amyloid in approximately 95% of patients afflicted with type II diabetes (*1*−*3*). IAPP has also been shown to be a toxic agent *in vitro* when added to human islet β-cells (*4*).

Many of the therapeutic strategies for preventing or slowing the progression of amyloid diseases such as type II diabetes involve slowing or preventing the aggregation of the amyloidogenic proteins. To this end, a great deal of effort has been made in identifying the amino acids responsible for the aggregation-prone nature of amyloidogenic peptides such as IAPP. Preventing IAPP aggregation, and hence the formation of the toxic oligomers and amyloid, could prevent disease progression.

It is well established that rodent IAPP (rIAPP) is nonamyloidogenic and nontoxic. It is also established that rats and mice are not known to develop type II diabetes (*5*). A comparison of the peptide sequences between human and rodent IAPP showed six amino acid substitutions (Figure 1). Five of the substitutions known to convert amyloidogenic human IAPP into nonamyloidogenic rodent IAPP occur in the 20−29 region of the peptide. Because of these substitutions the 20−29 region has long been described as the amyloidogenic region of IAPP (*6*−*8*). While recent studies have indicated that several mutations outside of the 20−29 region can hinder fibrillogenesis, the 20−29 region has been the focus of most studies aimed at preventing IAPP aggregation (*9*−*15*). These studies have provided a great deal of information about the aggregation-prone 20−29 region of IAPP. However, no extensive screen has been performed to identify nonamyloidogenic mutations of IAPP. A broad screen would not only identify individual mutants of IAPP that are nonamyloidogenic but could also pinpoint the interactions responsible for IAPP aggregation.

Here, we describe a screen that takes advantage of the slow folding kinetics of enhanced green fluorescent protein (EGFP) to select for IAPP mutations that resist aggregation. Proteins fused to the N-terminus of EGFP can attenuate the extent of EGFP fluorescence within a cell (*16*). This control over EGFP fluorescence is related to the ability of the fusion protein to remain monomeric and soluble in solution. Fusion proteins that self-assemble into insoluble fibrils prevent the EGFP from folding and fluorescing. In this screen the IAPP peptide was genetically fused to EGFP. When expressed in *Escherichia coli*, the IAPP−EGFP fusion protein produces virtually no green color or fluorescence due to the amyloidogenic nature of IAPP. Aggregation of IAPP precludes folding, and hence fluorescence, of the EGFP reporter. However, when a soluble and nonamyloidogenic mutant of IAPP is fused to EGFP, the EGFP is capable of folding and fluorescing. Using error-prone PCR, we constructed

†Funding by NIH Grant R15AG032582-01A1.
*Corresponding author. E-mail: dmoffet@lmu.edu. Tel: (310) 338-4400. Fax: (310) 338-2905.
[1]Abbreviations: IAPP, islet amyloid polypeptide; hIAPP, human IAPP; ThT, thioflavin T; IPTG, isopropyl β-D-1-thiogalactopyranoside; EGFP, enhanced green fluorescent protein; HFIP, hexafluoroisopropyl alcohol; DTT, dithiothreitol; AFM, atomic force microscope; NEB, New England Biolabs; SOC media, super optimal broth with catabolite repression; LB media, Luria−Bertani media.

Published on Web 08/10/2010

```
                          1    5    10          20          29        37
HUMAN IAPP                KCNTATCATQRLANFLVHSSNNFGAILSSTNVGSNTY
Monkey IAPP (34)          -------------------G-----------------
Cat                       ----------------IR----L-----P--------
hIAPP 3xL(10)             --------------L-------L-------------L
F15A (30)                 --------------A----------------------
F15S (30)                 --------------S----------------------
F15D (30)                 --------------D----------------------

Nonamyloidogenic
F15K (30)                 --------------K----------------------
Rat IAPP:                 -----------------R----L-PV-PP--------
I26P (11)                 -------------------------P-----------
hIAPP8-37 3xP(9)                ---------P-P----------P-------
N14L(13)                  ------------L------------------------
N21L(13)                  --------------------L---------------
```

FIGURE 1: Comparison of previously analyzed IAPP variants. Sequences known to aggregate are shown at the top. Sequences known to be nonamyloidogenic are shown in bold at the bottom. Only amino acid differences compared to wild-type human IAPP are indicated.

a library of mutated IAPP sequences genetically fused to EGFP. This mutated IAPP−EGFP library was expressed in *E. coli* and screened for green fluorescent colonies. Those colonies showing the greatest fluorescence were selected and identified through DNA sequencing. To verify the results, four of the selected IAPP mutant peptides were chemically synthesized and their propensity to aggregate and form fibers was characterized *in vitro*.

EXPERIMENTAL PROCEDURES

Materials. Synthetic peptides were prepared by GenScript Corp. (Piscataway, NJ), except for A13E IAPP (synthesized by Lifetein, LLC, South Plainfield, NJ). DNA purification kits were from Qiagen Inc. (Valencia, CA). Klenow fragment DNA polymerase and restriction endonucleases were from New England Biolabs (Ipswich, MA). Expand high fidelity DNA polymerase was from Roche . pET28a and pCDF-1b plasmids were from Stratagene. DNA sequencing was performed by Davis Sequencing, Inc. (Davis, CA).

Construction of the IAPP Gene. The IAPP gene was constructed using overlap gene assembly. Two single-stranded DNA oligonucleotides (Supporting Information) were designed to base pair to each other with complementary 3′-termini. Oligos were diluted to 10 μM with deionized H_2O (dI H_2O). Twenty-six microliters of oligo 1 and 26 μL of oligo 2 were mixed together in a sterile Eppendorf tube along with 25 μL of 10× Ecopol buffer (New England Biolabs) and 143 μL of dI H_2O. This solution was heated at 85 °C in a heat block for 15 min to fully denature the DNA oligonucleotides. The heat block was turned down to 37 °C to allow the mixture to slowly cool and allow proper annealing of the oligos. After the temperature dropped to 37 °C, 10 μL of 5 mM dNTP's, 10 μL of 20 mM DTT, and 4 μL of Klenow fragment (5000 units/mL; NEB) were added. The solution was incubated at 37 °C for 1 h. Double-stranded gene product was purified (Qiagen PCR purification kit). Codons were optimized for expression in *E. coli*. The full-length gene product was PCR amplified (Supporting Information). The gene product was digested with *Nco*I and *Bam*HI restriction endonucleases and ligated into analogously digested pAβ42-EGFP(*17*) yielding the final plasmid, pIAPP−EGFP.

Construction of the I26P Mutant of IAPP. The I26P variant of IAPP is known to be nonamyloidogenic and can inhibit IAPP fibril formation (*11*). As a positive control, we constructed the I26P mutant of IAPP and genetically fused it to EGFP. We used the QuikChange site-directed mutagenesis system (Stratagene) and the following primers: 5′-CAACAACTTTGGCGCG**CCG**CTGAGCAGCACCAACG-3′ and 5′-CGTTGGTGCTGCTCAG**CGG**CGCGCCAAAGTTGTTG-3′.

Construction of the Mutated IAPP Library. The mutated IAPP library was generated using PCR-based random mutagenesis (Stratagene/Agilent Technologies Genemorph II mutagenesis kit). The DNA primers used were 5′-CTTTAATAAGGAGATATACCATGGGC-3′ and 5′-GCGGAGCCAGCGGATCC-3′. These primers maintained the *Nco*I and *Bam*HI restrictions sites but allowed for mutagenesis of each of the 37 codons of the IAPP gene. Four cycles of PCR mutagenesis were performed (following instructions of the manufacturer) on the IAPP gene to yield an amplified gene product containing, on average, one mutation per gene. After the fourth round of amplification, the randomized gene mixture was digested with *Nco*I and *Bam*HI restriction endonucleases and ligated into similarly digested pAβ42-EGFP (*17*). The ligation product was purified with the Qiagen PCR purification kit and eluted with dI H_2O.

The mutated IAPP−EGFP plasmid library was transformed into electrocompetent XL1-Blue *E. coli* (*18*) and plated on LB media plates containing 20 μg/mL antibiotic streptomycin. The plates were incubated for 16 h at 37 °C. Approximately 25000 colonies were produced. Five colonies were randomly chosen for DNA sequencing to verify mutagenesis. Three of the five samples had mutations resulting in changes to the amino acid sequence (K1I, K1N, and the triple mutant H18N, A25V, L27N). One sample possessed a silent mutation that yielded the wild-type IAPP peptide sequence. The fifth sample was the wild-type IAPP. We estimate that 80% of the 25000 colonies generated contained at least one mutation. The colonies were scraped from the plates and combined in 100 mL of LB media containing 20 μg/mL streptomycin. The mutated IAPP−EGFP plasmid library was purified from this cell suspension using Qiagen's DNA purification miniprep kit.

Screening the Mutated IAPP−EGFP Library. The mutated IAPP−EGFP plasmid library DNA was transformed into electrocompetent BL21(DE3) *E. coli*. The cells were rescued with SOC media and plated on sterile nitrocellulose discs placed on LB media plates containing 20 μg/mL streptomycin. The transformation mixture was plated to yield a density of approximately 500 colonies per plate. The LB plates were incubated for 16 h at 37 °C. The nitrocellulose discs, covered in colonies, were transferred to LB media plates containing 20 μg/mL streptomycin and

2 mM IPTG. The plates were incubated at 37 °C for 4−6 h. To select green colonies, the plates were scanned both under white light and under 490 nm light. Green fluorescent colonies were selected based on their visual ability to fluoresce green.

Quantification of Cellular Fluorescence. Selected colonies were grown to an OD_{600} of 0.7 before protein induction with 1 mM IPTG. The induced *E. coli* were incubated at 37 °C with shaking for 4 h. The cells were transferred to black 96-well fluorometer plates to record the fluorescence emission (Ex_{490nm} and Em_{516nm}) of each culture using a Hitatchi F-7000 fluorescence spectrophotometer. To ensure expression of each variant, whole cell lysates were analyzed using SDS−PAGE. A 1 mL aliquot of cell culture was pelleted and the supernatant removed. The pellets were washed with 20 mM phosphate buffer, pH 7.2, and pelleted again. The washed pellets were resuspended in 200 μL of SDS−PAGE loading buffer and boiled for 10 min. Samples were centrifuged for 10 min at 13000*g*. Ten microliters of the supernatant for each variant was loaded onto a precast 4−20% gradient polyacrylamide gel (Bio-Rad) and analyzed via SDS−PAGE. Gels were stained with Coomassie Brilliant Blue R250 dye and destained with a solution of 7% methanol and 7% acetic acid.

Selected colonies were also visually compared by streaking each variant onto a sterile nitrocellulose disc placed on an LB media plate containing streptomycin (20 μg/mL). After incubating the plates for 16 h at 37 °C, the discs were transferred to fresh LB media plates containing streptomycin and 2 mM IPTG. Plates were incubated for 4−6 h at 37 °C. The plates were scanned using a Bio-Rad Molecular Imager VersaDoc MP imaging system.

Preparing Disaggregated IAPP. Synthetic IAPP (0.5 mg) (GenScript Corp.) or mutated IAPP (0.5 mg) (GenScript) was dissolved in 4.0 mL of hexafluoroisopropyl alcohol(HFIP) and placed in a sonicating water bath for 10 min. The solution was divided into 500 μL aliquots and stored at −80 °C.

Thioflavin T Assays. Each aliquot of disaggregated IAPP (from above) was thawed and the HFIP removed over a stream of dry nitrogen gas. The resulting solid was dissolved in 20 mM Tris buffer, pH 7.40, to 10.6 μM. The samples were incubated at 37 °C with shaking (200 rpm). Forty microliters of each sample was removed at indicated time points and mixed with 660 μL of 31 μM thioflavin T in 20 mM Tris buffer, pH 7.40. The thioflavin T mixture was incubated at room temperature in the dark for 5 min before recording the thioflavin T fluorescence (Ex_{450nm} and Em_{488nm}) using a Hitatchi F-7000 fluorescence spectrophotometer 96-well plate reader.

Atomic Force Microscope. Each aliquot (from above) was thawed and the HFIP removed over a stream of dry nitrogen gas. The resulting solid was dissolved in 20 mM Tris buffer, pH 7.40, to 106 μM. The samples were incubated at 37 °C with shaking (200 rpm). Five microliters was taken from each sample at various time points, diluted 5-fold in filtered dI H_2O, and added directly to freshly cleaved mica. After 15 min of incubation, the mica surface was washed with 200 μL of filtered dI H_2O and allowed to air-dry. Samples were scanned using an MFP-3D atomic force microscope (Asylum Research) set on A/C mode and a 240 μm silicon cantilever (Olympus).

RESULTS

Error-prone PCR was used to construct a library of mutated IAPP sequences genetically fused to the reporter protein EGFP.

```
                        1   5    10         20        29       37
HUMAN IAPP:             KCNTATCATQRLANFLVHSSNNFGAILSSTNVGSNTY
K1I                     I-----------------------------------
K1N                     N-----------------------------------
H18N, A25V, L27N        ----------------N------V-N----------

Nonamyloidogenic
S28G:                   ---------------------------G---------
L27R                    --------------------------R----------
I26D:                   -------------------------D-----------
I26T                    ------------------------T------------
L16M                    ---------------M--------------------
L16Q                    ---------------Q--------------------
N21D                    --------------------D----------------
V17G                    ----------------G--------------------
L27Q                    --------------------------Q----------
A13E                    ------------E------------------------
L12P                    -----------P-------------------------
R11P                    ----------P--------------------------
V17E                    ----------------E--------------------
F15C                    --------------C----------------------
C7R                     ------R-------------------------------
Q10H                    ---------H--------------------------
C2Y                     -Y-----------------------------------
V32A                    -------------------------------A-----
A8D                     -------D-----------------------------
N21K                    --------------------K----------------
N31S                    -----------------------------S------
T4S                     ---S---------------------------------

F23I,L27P:              ----------------------I---P----------
A13G,S20G               ------------G------G-----------------
V17E, N35I              ----------------E-----------------I--
N31D, N35Δ              -------------------------------D--- --

F15I, V17E, S28N        --------------I-E----------N---------
A25S, S28T, S29T        ------------------------S--TT--------
```

FIGURE 2: Comparison of IAPP variants identified through the use of the mutated IAPP−EGFP screen. Amyloidogenic sequences are listed at the top. Nonamyloidogenic sequences are indicated in bold lettering at the bottom. Only amino acid residues that differ from human IAPP are indicated.

This library was transformed into electrocompetent BL21(DE3) *E. coli*. These transformations resulted in approximately 25000 individual colonies, of which approximately 20000 possessed at least one mutation. Visual scanning of the plates under both white light and 490 nm wavelength light identified 87 colonies with significant green fluorescence. These bright colonies were selected and their DNA sequenced (Davis Sequencing). Fifty-nine of the selected colonies possessed deletions that resulted in truncated IAPP sequences (typically fewer than 15 amino acids fused to EGFP), yet remained in the correct reading frame to yield active EGFP. The remaining samples expressed a full-length IAPP sequence. Twenty-two of the selected full-length IAPP sequences possessed a single mutation, four possessed double mutations, and two possessed triple mutations (Figure 2).

The level of green fluorescence for each of the selected colonies was compared to that of wild-type human IAPP fused to EGFP. The selected colonies were also compared to the nonamyloidogenic I26P mutant of IAPP fused to EGFP (*11*). For a visual comparison, selected variants were grown on nitrocellulose discs and incubated with IPTG to induce protein expression (Figure 3). For a more quantitative comparison, each variant was grown in LB liquid media and induced with IPTG. The resulting EGFP fluorescence was detected using a Hitatchi F-7000 fluorescence spectrophotometer (Figure 4). To ensure comparable expression of each IAPP−EGFP variant, whole cell lysates were analyzed with SDS−PAGE (Figure 5).

The use of fluorescent protein fusions to amyloidogenic proteins has been shown to be an effective method for distinguishing relative levels of amyloidogenicity (*17*, *19*−*24*). However, it is important to verify the results of any screen to demonstrate the validity of the selected samples. To this end, we chose four of the selected variants,

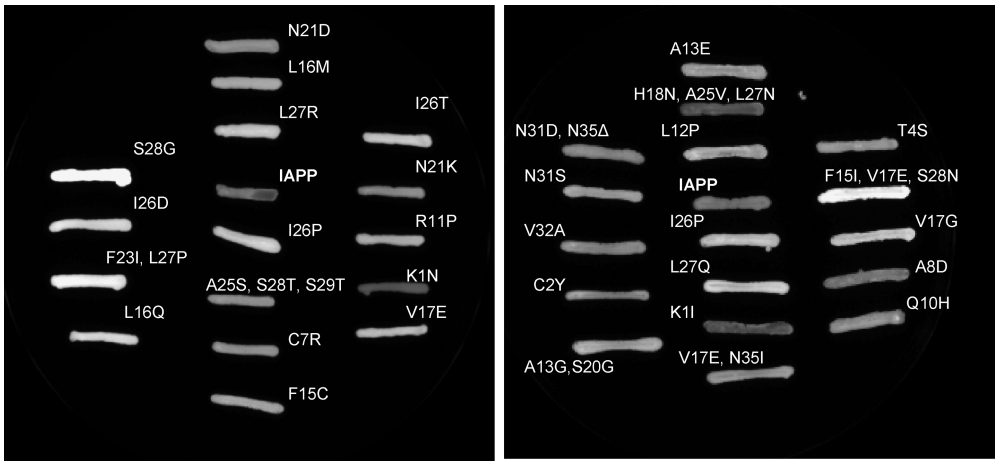

FIGURE 3: Visual comparison of selected IAPP−EGFP variants to wild-type human IAPP fused to EGFP (IAPP in center of each panel) and to the nonamyloidogenic variant I26P. The CCD camera detector does not show data in color. Data are shown as fluorescence emission intensity.

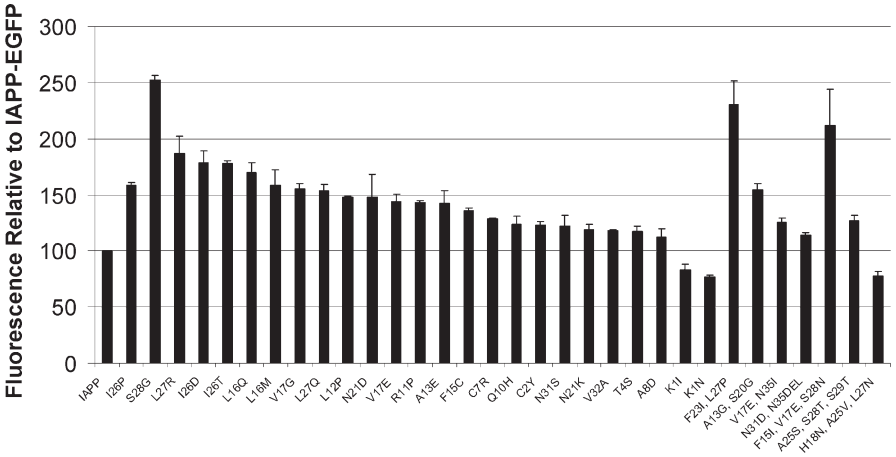

FIGURE 4: Quantitative comparison of selected IAPP−EGFP variants. Fluorescence intensity of wild-type human IAPP fused to EGFP was set at 100% fluorescence. The fluorescence intensity of each variant was plotted as a percentage of the fluorescence of wild-type human IAPP. Variants with a relative fluorescence of 100% or less are considered to be amyloidogenic.

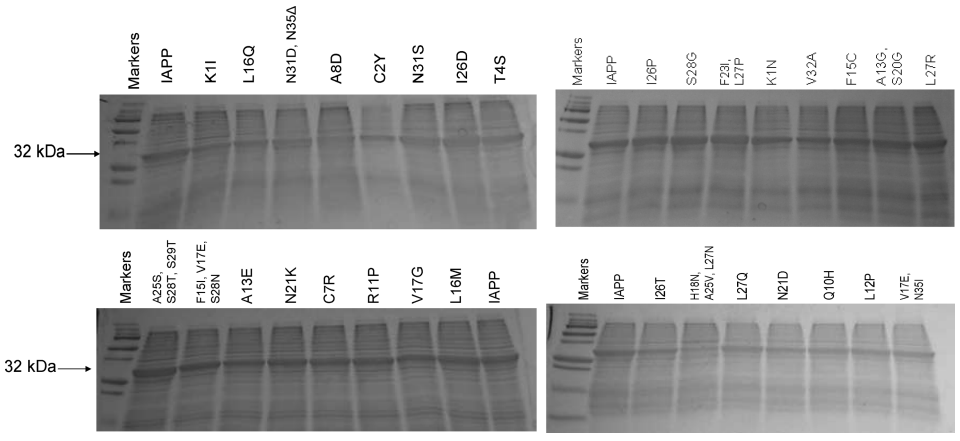

FIGURE 5: Comparison of expression of 32 kDa IAPP−EGFP variants in BL21(DE3) *E. coli*. Each variant showed an expression level comparable to that of wild-type IAPP fused to EGFP (labeled as IAPP in each gel).

S28G, I26D, A13E, and L16Q, to be chemically synthesized and experimentally characterized for their propensity to aggregate. We chose to characterize the S28G and I26D variants due to their elevated EGFP fluorescence. Because several nonamyloidogenic variants were identified having one or more mutations in the A13-V17 region, we chose to also characterize the L16Q and A13E variants.

The ability of the four selected variants to bind thioflavin T (ThT), an indicator of amyloid aggregation, was compared to that of wild-type IAPP. Human IAPP is one of the most amyloidogenic peptides known. To characterize the selected variants' ability to resist aggregation, we subjected each variant to conditions known to quickly promote aggregation. Samples were incubated at 10 μM

concentration (Figure 6) and at 100 μM (Supporting Information Figure 1S), with vigorous shaking at 37 °C. Under these conditions, wild-type IAPP began to aggregate, and hence bind ThT, within minutes of incubation. The decrease in ThT fluorescence after reaching its maximum is commonly witnessed in these assays and is consistent with previously reported amyloid aggregation reactions (*25*, *26*).

The mutated IAPP samples selected to resist aggregation showed drastically reduced ThT fluorescence compared to IAPP.

The ability of the synthetic mutant IAPP variants to form fibers was compared to wild-type human IAPP (Figure 7) using atomic force microscopy (AFM). All IAPP samples were incubated under conditions known to promote fiber formation. Only wild-type IAPP was found to form fibers. The selected variants

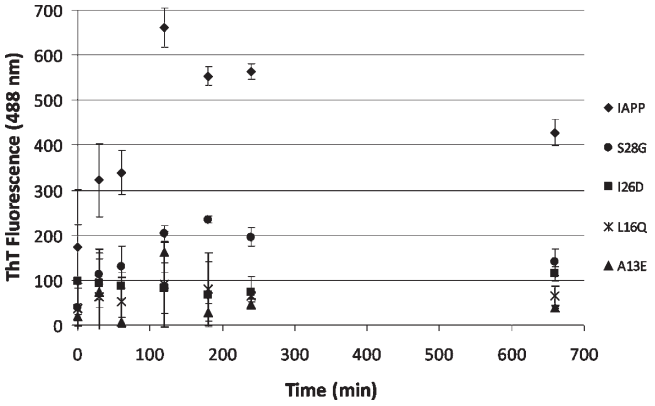

FIGURE 6: Comparison of thioflavin T binding time course by selected variants and wild-type human IAPP. One representative time experiment is shown with the error bars representing the standard deviation of all trials ($n \geq 3$).

I26D, S28G, A13E, and L16Q were not found to form fibers under any of the conditions tested.

DISCUSSION

Many of the sequences selected with this screen were found to have mutations within the 20−29 region of IAPP. This is commonly referred to as the amyloidogenic region of IAPP (*6*, *8*, *9*, *11*). In this screen, 11 of the 28 variants selected had at least one mutation within the 20−29 region of IAPP. Recent work also indicates that the amyloidogenic region could be extended to include the 30−33 region of IAPP (*9*, *14*). Indeed, we find that 14 of the 28 sequences selected had mutations within the 20−33 region of IAPP. These results are consistent with previous studies that indicate the 20−33 region as being important for IAPP aggregation.

Seven of the 28 sequences selected with this screen contained at least one mutation within the 15−17 region of IAPP (the amino acids FLV). There is little evidence within the current literature to indicate these amino acids as being amyloidogenic. Gazit and co-workers make several arguments suggesting a role for the amyloidogenic nature of the 14−19 region (*27*−*29*), but the majority of work focuses on the 20−29 region as being responsible for amyloidogenicity. Because 25% of the selected nonamyloidogenic sequences from this screen have at least one FLV mutation, these amino acids may be important for IAPP aggregation. The selected variants with mutations outside the 20−33 region (such as the L16Q mutant) were resistant to aggregation despite the amyloidogenic nature of the 20−33 region of IAPP.

Our results suggest the 15−17 region of IAPP (amino acids FLV) is important for the aggregation of IAPP. Eisenberg and co-workers recently determined the crystal structure of an IAPP

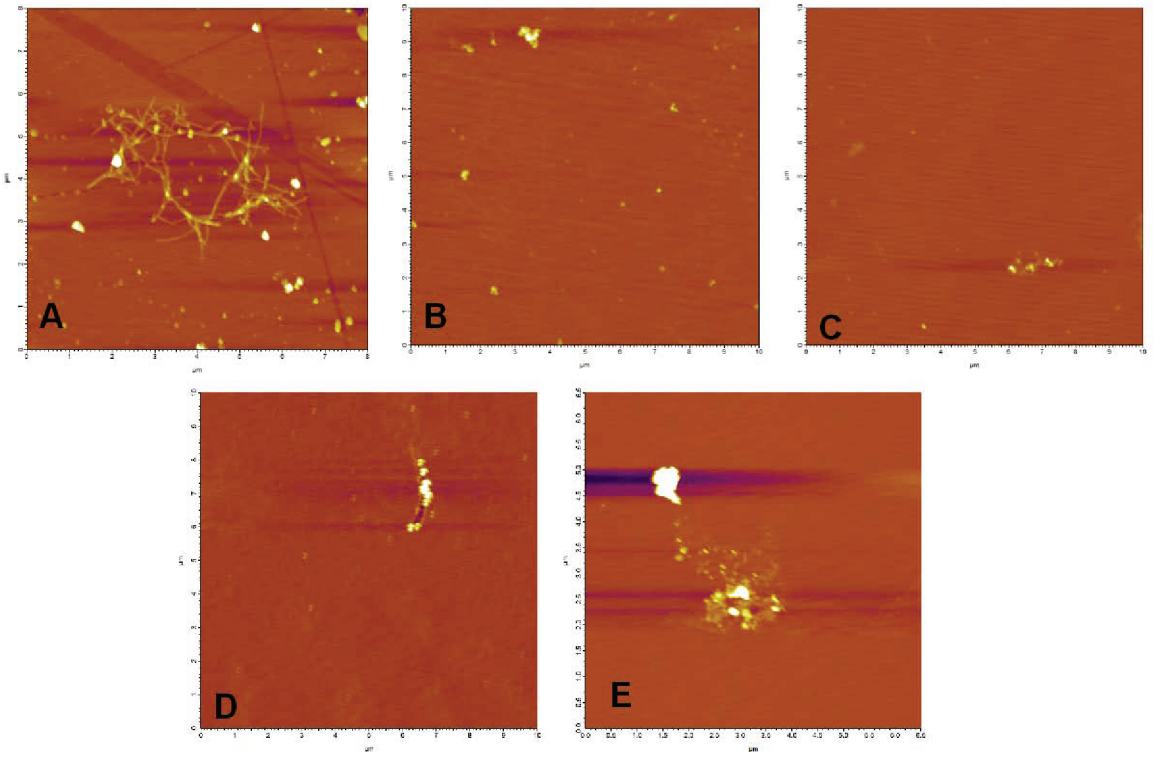

FIGURE 7: AFM images of (A) IAPP, (B) I26D, (C) S28G, and (D) L16Q after 30 min of incubation at 37 °C with agitation and (E) A13E after 60 min of incubation at 37 °C with agitation. Time points shown were selected based on maximum ThT binding as determined in Figure 1S. Each variant was tested at multiple time points. Fibers were not detected under any of the conditions tested for the selected mutant variants (while wild-type IAPP was found to produce fibers under all conditions tested and at all time points after 15 min of incubation).

fusion to maltose binding protein (MBP) (*30*). In their model, they show the FLV region of IAPP as the core of a helix thought to be associated with IAPP aggregation (*31*−*33*). This model shows the FLV region of IAPP associating with the YLV region of insulin B chain (*30*). Based on these models, and the results of our screen, the FLV region appears to be an important part of IAPP aggregation. Interestingly, the amyloid peptide associated with Alzheimer's disease, Aβ, contains an LVF sequence in its putative aggregation region.

Alanine 13 was found to be an additional amino acid of interest selected from this screen. Ala13 is in the middle of the putative helical region of IAPP, believed to play a role in aggregation. Our screen identified two Ala13 mutants, A13E and the double mutant A13G, S20G, as being resistant to amyloid aggregation. The lack of aggregation witnessed with the A13E mutation could be attributed to the drastic change of a small alanine for a large negatively charged glutamic acid. However, the double mutant A13G, S20G could be more informative about the role of A13 in IAPP aggregation. Previous studies have shown that S20G (which is found in primates) is a highly amyloidogenic sequence (*34*). Because the A13G, S20G double mutant was nonamyloidogenic according to our screen, and the S20G single mutation (as found in primates) remains amyloidogenic, we assign the lack of amyloidogenicity of this double mutant as being due to the A13G mutation. It is believed that this region of IAPP folds into an α-helix which may be important for aggregation (*33*). Because glycine is a strong helix breaker, the observed results with the A13G variant support the theory that this region of IAPP adopts a helical structure on the pathway to aggregation (*33*). Decreasing this region's ability to adopt a helical fold may have resulted in the observed lack of fiber formation and decreased ThT binding of the A13G, S20G variant.

Previous studies have shown that amyloid aggregation and fiber formation have a pH dependence (*35*−*38*). Many amyloid proteins become more aggregation prone as the solution pH nears the isoelectric point (p*I*) of the protein. Wild-type IAPP, L16Q, and S28G have an identical p*I* of 8.90, yet the L16Q and S28G variants were resistant to aggregation. This suggests that the resistance to aggregation is not due to pH effects of the solution but rather to specific protein−protein interactions. The p*I* of the A13E and I26D variants are both 8.05. Because the p*I* of A13E and I26D is closer to the pH of the solution (pH = 7.4) than that of wild-type IAPP, we would expect those variants to be more prone to aggregate. Again, the lack of aggregation of these two peptides cannot be attributed solely to the pH of the solution but are likely due to protein−protein interactions.

Several programs have been developed to identify *in silico* the amyloidogenic regions of proteins. We used one such program, TANGO (http://tango.crg.es) (*38*−*40*), to analyze the IAPP and mutant IAPP sequences. Tango identified two aggregation-prone regions in the IAPP peptide sequence, amino acids L12−V17 and amino acids F23−L27. According to TANGO, both the A13E and L16Q mutations eliminate the L12−V17 amyloidogenic region (but have no effect on the F23−L27 region). Likewise, TANGO indicated that the I26D mutation eliminates the F23−L27 amyloidogenic region (but has no effect on the L12−V17 region). The results of the TANGO program support our experimental data in indicating that A13 and F15−V17 are important regions for the overall amyloidogenicity of IAPP.

Several mutant variants are consistent with previously published reports. In IAPP, the disulfide bond between Cys2 and Cys7 has been identified as an important contributor of fiber formation (*41*). Two variants identified as nonamyloidogenic in our screen were C2Y and C7R. These mutations would both result in the loss of this intramolecular disulfide bond and, hence, would be expected to be less amyloidogenic.

This EGFP based screen provided a facile method for sampling large numbers of sequence variants to identify those that resist amyloid aggregation. The screen is predicated on the fact that EGFP is a relatively slow-folding enzyme in prokaryotic expression (*42*). This slow EGFP folding time allows the amyloidogenic peptides to aggregate prior to EGFP folding and fluorescence. Sequences selected through this screen should prove to be nonamyloidogenic or, at the least, should take longer to aggregate than EGFP takes to fold and fluoresce. The four synthetic variants tested (I26D, S28G, A13E, and L16Q) showed decreased levels of ThT fluorescence and did not form fibers under the conditions tested. We believe these results are consistent with previously reported results that the 20−33 region of IAPP is amyloidogenic. However, this work indicates that other regions of the IAPP sequence, FLV (residues 15−17) and Ala13, should be considered important for amyloidogenesis.

SUPPORTING INFORMATION AVAILABLE

Oligonucleotide primers and one figure as described in the text. This material is available free of charge via the Internet at http://pubs.acs.org.

REFERENCES

1. Apostolidou, M., Jayasinghe, S. A., and Langen, R. (2008) Structure of alpha-helical membrane-bound human islet amyloid polypeptide and its implications for membrane-mediated misfolding. *J. Biol. Chem. 283*, 17205–17210.
2. Hull, R. L., Westermark, G. T., Westermark, P., and Kahn, S. E. (2004) Islet amyloid: A critical entity in the pathogenesis of type 2 diabetes. *J. Clin. Endocrinol. Metab. 89*, 3629–3643.
3. Kahn, S. E., Andrikopoulos, S., and Verchere, C. B. (1999) Islet amyloid: A long-recognized but underappreciated pathological feature of type 2 diabetes. *Diabetes 48*, 241–253.
4. Ritzel, R. A., Meier, J. J., Lin, C. Y., Veldhuis, J. D., and Butler, P. C. (2007) Human islet amyloid polypeptide oligomers disrupt cell coupling, induce apoptosis, and impair insulin secretion in isolated human islets. *Diabetes 56*, 65–71.
5. Matveyenko, A. V., and Butler, P. C. (2006) Islet amyloid polypeptide (IAPP) transgenic rodents as models for type 2 diabetes. *ILAR J. 47*, 225–233.
6. Westermark, P., Engstrom, U., Johnson, K. H., Westermark, G. T., and Betsholtz, C. (1990) Islet amyloid polypeptide—Pinpointing amino-acid-residues linked to amyloid fibril formation. *Proc. Natl. Acad. Sci. U.S.A. 87*, 5036–5040.
7. Nanga, R. P., Brender, J. R., Xu, J., Veglia, G., and Ramamoorthy, A. (2008) Structures of rat and human islet amyloid polypeptide IAPP(1−19) in micelles by NMR spectroscopy. *Biochemistry 47*, 12689–12697.
8. Gazit, E. (2005) Mechanisms of amyloid fibril self-assembly and inhibition. *FEBS J. 272*, 5971–5978.
9. Abedini, A., and Raleigh, D. P. (2006) Destabilization of human IAPP amyloid fibrils by proline mutations outside of the putative amyloidogenic domain: Is there a critical amyloidogenic domain in human IAPP? *J. Mol. Biol. 355*, 274–281.
10. Marek, P., Abedini, A., Song, B. B., Kanungo, M., Johnson, M. E., Gupta, R., Zaman, W., Wong, S. S., and Raleigh, D. P. (2007) Aromatic interactions are not required for amyloid fibril formation by islet amyloid polypeptide but do influence the rate of fibril formation and fibril morphology. *Biochemistry 46*, 3255–3261.
11. Abedini, A., Meng, F. L., and Raleigh, D. P. (2007) A single-point mutation converts the highly amyloidogenic human islet amyloid polypeptide into a potent fibrillization inhibitor. *J. Am. Chem. Soc. 129*, 11300.
12. Abedini, A., and Raleigh, D. P. (2005) The role of His-18 in amyloid formation by human islet amyloid polypeptide. *Biochemistry 44*, 16284–16291.

13. Koo, B. W., Hebda, J. A., and Miranker, A. D. (2008) Amide inequivalence in the fibrillar assembly of islet amyloid polypeptide. *Protein Eng., Des. Sel. 21*, 147–154.
14. Scrocchi, L. A., Chen, Y., Waschuk, S., Wang, F., Cheung, S., Darabie, A. A., McLaurin, J., and Fraser, P. E. (2002) Design of peptide-based inhibitors of human islet amyloid polypeptide fibrillogenesis. *J. Mol. Biol. 318*, 697–706.
15. Tracz, S. M., Abedini, A., Driscoll, M., and Raleigh, D. P. (2004) Role of aromatic interactions in amyloid formation by peptides derived from human Amylin. *Biochemistry 43*, 15901–15908.
16. Waldo, G. S., Standish, B. M., Berendzen, J., and Terwilliger, T. C. (1999) Rapid protein-folding assay using green fluorescent protein. *Nat. Biotechnol. 17*, 691–695.
17. Baine, M., Georgie, D. S., Shiferraw, E. Z., Nguyen, T. P. T., Nogaj, L. A., and Moffet, D. A. (2009) Inhibition of A beta 42 aggregation using peptides selected from combinatorial libraries. *J.Pept. Sci. 15*, 499–503.
18. Sharma, R. C., and Schimke, R. T. (1996) Preparation of electrocompetent *E. coli* using salt-free growth medium. *BioTechniques 20*, 42–44.
19. de Groot, N. S., Aviles, F. X., Vendrell, J., and Ventura, S. (2006) Mutagenesis of the central hydrophobic cluster in A beta 42 Alzheimer's pepticle—Side-chain properties correlate with aggregation propensities. *FEBS J. 273*, 658–668.
20. Kim, W., Kim, Y., Min, J., Kim, D. J., Chang, Y. T., and Hecht, M. H. (2006) A high-throughput screen for compounds that inhibit aggregation of the Alzheimer's peptide. *ACS Chem. Biol. 1*, 461–469.
21. Wurth, C., Guimard, N. K., and Hecht, M. H. (2002) Mutations that reduce aggregation of the Alzheimer's Abeta42 peptide: An unbiased search for the sequence determinants of Abeta amyloidogenesis. *J. Mol. Biol. 319*, 1279–1290.
22. Wurth, C., Kim, W., and Hecht, M. H. (2006) Combinatorial approaches to probe the sequence determinants of protein aggregation and amyloidogenicity. *Protein Pept. Lett. 13*, 279–286.
23. Kim, W., and Hecht, M. H. (2006) Generic hydrophobic residues are sufficient to promote aggregation of the Alzheimer's A beta 42 peptide. *Proc. Natl. Acad. Sci. U.S.A. 103*, 15824–15829.
24. Kim, W., and Hecht, M. H. (2008) Mutations enhance the aggregation propensity of the Alzheimer's A beta peptide. *J. Mol. Biol. 377*, 565–574.
25. Yamin, G., Ruchala, P., and Teplow, D. B. (2009) A peptide hairpin inhibitor of amyloid beta-protein oligomerization and fibrillogenesis. *Biochemistry 48*, 11329–11331.
26. Ahn, J. S., Lee, J. H., Kim, J. H., and Paik, S. R. (2007) Novel method for quantitative determination of amyloid fibrils of alpha-synuclein and amyloid beta/A4 protein by using resveratrol. *Anal. Biochem. 367*, 259–265.
27. Gilead, S., and Gazit, E. (2008) The role of the 14−20 domain of the islet amyloid polypeptide in amyloid formation. *Exp. Diabetes Res. 2008*, 256954.
28. Gilead, S., Wolfenson, H., and Gazit, E. (2006) Molecular mapping of the recognition interface between the islet amyloid polypeptide and insulin. *Angew. Chem., Int. Ed. Engl. 45*, 6476–6480.
29. Mazor, Y., Gilead, S., Benhar, I., and Gazit, E. (2002) Identification and characterization of a novel molecular-recognition and self-assembly domain within the islet amyloid polypeptide. *J. Mol. Biol. 322*, 1013–1024.
30. Wiltzius, J. J. W., Sievers, S. A., Sawaya, M. R., and Eisenberg, D. (2009) Atomic structures of IAPP (amylin) fusions suggest a mechanism for fibrillation and the role of insulin in the process. *Protein Sci. 18*, 1521–1530.
31. Williamson, J. A., Loria, J. P., and Miranker, A. D. (2009) Helix stabilization precedes aqueous and bilayer-catalyzed fiber formation in islet amyloid polypeptide. *J. Mol. Biol. 393*, 383–396.
32. Williamson, J. A., and Miranker, A. D. (2007) Direct detection of transient alpha-helical states in islet amyloid polypeptide. *Protein Sci. 16*, 110–117.
33. Yonemoto, I. T., Kroon, G. J., Dyson, H. J., Balch, W. E., and Kelly, J. W. (2008) Amylin proprotein processing generates progressively more amyloidogenic peptides that initially sample the helical state. *Biochemistry 47*, 9900–9910.
34. Sakagashira, S., Hiddinga, H. J., Tateishi, K., Sanke, T., Hanabusa, T., Nanjo, K., and Eberhardt, N. L. (2000) S20G mutant amylin exhibits increased in vitro amyloidogenicity and increased intracellular cytotoxicity compared to wild-type amylin. *Am. J. Pathol. 157*, 2101–2109.
35. Hortschansky, P., Schroeckh, V., Christopeit, T., Zandomeneghi, G., and Fandrich, M. (2005) The aggregation kinetics of Alzheimer's beta-amyloid peptide is controlled by stochastic nucleation. *Protein Sci. 14*, 1753–1759.
36. Chiti, F., Stefani, M., Taddei, N., Ramponi, G., and Dobson, C. M. (2003) Rationalization of the effects of mutations on peptide and protein aggregation rates. *Nature 424*, 805–808.
37. Nielsen, L., Khurana, R., Coats, A., Frokjaer, S., Brange, J., Vyas, S., Uversky, V. N., and Fink, A. L. (2001) Effect of environmental factors on the kinetics of insulin fibril formation: Elucidation of the molecular mechanism. *Biochemistry 40*, 6036–6046.
38. Fernandez-Escamilla, A. M., Rousseau, F., Schymkowitz, J., and Serrano, L. (2004) Prediction of sequence-dependent and mutational effects on the aggregation of peptides and proteins. *Nat. Biotechnol. 22*, 1302–1306.
39. Linding, R., Schymkowitz, J., Rousseau, F., Diella, F., and Serrano, L. (2004) A comparative study of the relationship between protein structure and beta-aggregation in globular and intrinsically disordered proteins. *J. Mol. Biol. 342*, 345–353.
40. Rousseau, F., Schymkowitz, J., and Serrano, L. (2006) Protein aggregation and amyloidosis: Confusion of the kinds? *Curr. Opin. Struct. Biol. 16*, 118–126.
41. Koo, B. W., and Miranker, A. D. (2005) Contribution of the intrinsic disulfide to the assembly mechanism of islet amyloid. *Protein Sci. 14*, 231–239.
42. Chang, H. C., Kaiser, C. M., Hartl, F. U., and Barral, J. M. (2005) De novo folding of GFP fusion proteins: High efficiency in eukaryotes but not in bacteria. *J. Mol. Biol. 353*, 397–409.